*Paulcy Rani Palayyan Raja Bai[1,*], Vaishnavi Sreekala Kumari Gopakumar[1], Sivakala Sarojam[2], Anu Mini Aravind[3], Xavier Thankappan Suryabai[3]*

*[1]Department of Chemistry, Government College for Women, Thiruvananthapuram 14, Kerala, [2]Department of Chemistry, Sree Narayana College, Chempazhanthy, Thiruvananthapuram, Kerala, [3]Centre for advanced materials research, Department of Physics, Government College for Women, Thiruvananthapuram 14, Kerala*

Scientific paper
ISSN 0351-9465, E-ISSN 2466-2585
https://doi.org/10.62638/ZasMat1059

Zastita Materijala 65 (3)
501 - 509 (2024)

# Microwave assisted synthesis of $NiMn_2O_4$ as electrode material for super capacitor applications

## ABSTRACT

*In this work, spinel $NiMn_2O_4$ was successfully synthesized through microwave assisted co-precipitation method and followed by calcination at 500°C. The crystal structure and the presence of functional groups in $NiMn_2O_4$ were characterized through X-ray diffraction (XRD) and Fourier transform infrared spectroscopy (FT-IR). The surface morphology was examined by field emission scanning electron microscopy (FE SEM). From the BET analysis surface area and average pore diameter of the mesoporous NMO nanoparticles are calculated to be 10.513 $m^2g^{-1}$and 8.55nm. The electrochemical performance of material as electrode material for supercapacitor applications was analysed by cyclic voltammetry (CV) and electrochemical impedance spectroscopy (EIS). The specific capacitance of the NMO electrode increased from 290.56 F/g to 751.57F/g with increase concentration from IM KOH to 6M KOH at scan rate of 5mV/s. These results indicate spinel $NiMn_2O_4$ as a promising candidate for high performance energy storage applications.*

***Keywords**: Microwave method, spinel, $NiMn_2O_4$, electrochemical performance, specific capacitance*

## 1. INTRODUCTION

Renewable, clean and ecofriendly energy resources are achieving foremost importance in order to address the global energy crisis and environmental pollution due to the consumption of fossil fuels. To fulfil this constantly increasing energy demands, there is a need of some portable and flexible electronic devices having convenient energy storage capacities with superior energy and power densities. In this regard supercapacitors, rechargeable batteries and fuel cells are designed as efficient energy storage devices to meet the present and future energy requirements [1]. Among these electrochemical based technologies, supercapacitors attracted more attention due to their higher power density, outstanding cycle life, high specific capacitance, safe functioning, and low maintenance cost [2,3]. Supercapacitors have versatile application in energy backup system, portable electronic devices and electrical vehicles [4].

Supercapacitors are classified into three based on the energy storage mechanism. Electrochemical double-layer capacitors (EDLCs), pseudo capacitors and hybrid supercapacitors. EDLCs can store charge either electrostatically or through non-faradic process, which involves no transfer of charge between electrode and electrolyte [5,6]. Carbon based materials such as graphene oxide (GO) [7], reduced graphene oxide(rGO) [8], carbon nanotubes (CNTs) [9] and carbon quantum dots (CQDs) [10] belongs to EDLCs type supercapacitor. Pseudo capacitors store charge via faradic process, which involves oxidation and reduction reactions take place between electrode and electrolyte, resulting in the charge transportation [11]. Conducting polymers and transition metal oxides $RuO_2$, NiO, CuO, $TiO_2$, $MnO_2$, $V_2O_5$, $Mn_3O_4$, $Fe_2O_3$ and $Co_3O_4$ belong to these types. Transition metal oxides have been widely explored for supercapacitor applications due to their layered structure and multiple oxidation states. Among the transition metal oxides $RuO_2$ considered to be the best pseudo capacitive material for supercapacitor electrodes due to very high specific capacitance, long cycle life, large potential window and remarkably high conductivity compared to other transition metal oxides, but the high cost and environmental issues limit its

*Corresponding author: Paulcy Rani P R
E-mail address:pr.paulcyrani@gmail.com
Paper received: 25. 02. 2024.
Paper corrected: 12. 05. 2024.
Paper accepted: 27. 05. 2024.
Paper is available on the website: www.idk.org.rs/journal

application [12]. Hybrid capacitors consist of both EDLC and redox mechanism, which enhances the power density as well as energy density. In hybrid supercapacitors, both physical and chemical processes are responsible for charge storage, and they are the evolved from EDLC and pseudo-capacitors to overcome various drawbacks of single mechanisms.

Nanostructured mixed transition metal oxides (MTMOs) such as $CuCo_2O_4$, $ZnCo_2O_4$, and $NiCo_2O_4$ have gained significant attention as working electrode materials, since they deliver rich redox activity and high surface area which provide exposed storage surface sites and the multiple oxidation states of metal ions that allow efficient faradaic reactions [13]. Out of the different MTMOs, considerable attention has been centred towards the synthesis of spinel $NiMn_2O_4$ (NMO) as it offers high conductivity, outstanding electrochemical capacitance, high redox-active sites, and exceptional chemical stability for energy storage applications [14]. Sahoo et al. reported the Cs of 194 F $g^{-1}$ from $NiMn_2O_4$ at the current density of 1 A/g[15]. Zhang et al. synthesized a porous $NiMn_2O_4$ by an epoxide-driven sol−gel process that exhibited a specific capacitance of 243 $Fg^{-1}$ at a scan rate of 5 $mVs^{-1}$ in 1 M $Na_2SO_4$ electrolyte [16]. Pang et al. also studied the electrochemical energy storage performance of porous $NiMn_2O_4$ via calcination of oxalate precursors, which showed a specific capacitance of 180 $Fg^{-1}$ at 250$mAg^{-1}$ current density [17]. In the present work, $NiMn_2O_4$(NMO) is synthesised by microwave assisted co-precipitation. The working electrodes are prepared from the synthesised spinel NMO. The electrochemical performance of the NMO nanoparticles has been evaluated in KOH electrolyte at 1M, 3M and 6M concentration.

## 2. EXPERIMENTAL DETAILS

### *2.1. Synthesis of NMO NPs by microwave assisted co-precipitation method*

NMO nanoparticles were prepared through microwave assisted co-precipitation method. 0.5 molar solutions of Manganese (II)chloride and Nickel (II)chloride were mixed and was stirred in a magnetic stirrer for 15 minutes. The molar ratio of metal cations Ni: Mn was maintained at 1:2 in the solution. Then 1M NaOH is added to the metal salt solution. After the complete addition of NaOH, it is then heated for 10 minutes in a microwave oven. The obtained mixed metal hydroxide is cooled, filtered and dried in an air oven at 80$^{o}$C for 24 hours. The mixed metal hydroxide is converted into mixed metal oxide, $NiMn_2O_4$(NMO) by heating it in a muffle furnace at 500$^{o}$C for 5 hours.

### *2.2 Characterizations*

The functional groups present in the sample are analysed using FT-IR spectroscopy, performed in Perkin-Elmer 'Spectrum Two' FT-IR Spectrometer. X-ray diffraction (XRD) studies of the NMO was done by Rigaku Miniflex-600 benchtop diffractometer with a Cu Kα radiation source (λ = 1.542 Å) in the range 10−90°. The chemical composition is studied by XPS analysis performed in Thermofisher Scientific ESCA- Lab, X- ray photoelectron Spectrometer. The surface morphology of the sample is analysed using FESEM with EDX (CARL ZEISS USA, resolution 1.5nm). BET (Brunauer-Emmett-Teller) and BJH (Barrett, Joyner, and Halenda) analyses (Altamira Instruments, Inc) were carried out to evaluate surface area and pore size distribution using nitrogen adsorption-desorption isotherms. The Electrochemical tests are performed in BioLogic VSP electrochemical workstation with three electrode system. Nickel foam casted with the active material ($NiMn_2O_4$) act as the working electrode, while platinum wire and Ag/AgCl electrode are used as counter and reference electrodes respectively.

### *2.3. Fabrication of working electrode and electrochemical study*

Before the preparation of electrode, the Ni-foam (1 cm X 1 cm) was cleaned with detergent, ethanol, concentrated hydrochloric acid and washed several times with DI water to eliminate the impurities and surface oxidant contents. To prepare the working electrodes, the electrode material (80%), polyvinylidene fluoride binder (10%) and carbon black (10%) were first mixed together using a mortar-pestle to make slurry, using N-methyl-2-pyrrolidinone solvent. This slurry was drop casted into Ni-foam (1 cm X 1 cm) and dried at 120$^{\circ}$C for 5 hours. The prepared electrodes were used for electrochemical characterizations.

The electrochemical performance of the prepared electrode material was tested through CV techniques. The electrochemical tests are performed in BioLogic VSP electrochemical workstation with three electrode system. Nickel foam casted with an active electrode material ($NiMn_2O_4$) act as working electrode, while Platinum wire and Ag/AgCl electrode are used as counter and reference electrodes respectively. The CV measurements were carried over a potential window -0.4 to 0.6V in KOH aqueous electrolyte in different concentration at scan rate from 5 mV/s to 100 mV/s. EIS measurement was carried over wide frequency range of 200KHz to 100mHz applying an AC voltage of 1 mV.

## 3. RESULTS AND DISCUSSIONS

### *3.1. FT-IR analysis*

The FT-IR spectra of $NiMn_2O_4$ is shown in (Fig. 1). A broad peak at 3435 $cm^{-1}$which can be attributed to O–H vibration and signifies that absorbed moisture exists at the surface of the NMO nanoparticles. The intense band observed at 582 $cm^{-1}$ attributed to the vibration of Ni-O atoms in the tetrahedral group, whereas the band at 497 $cm^{-1}$ assigned to the vibrational mode of Ni-Mn-O atoms [18] FT-IR analysis revealed the presence of spinel NMO in the synthesized material.

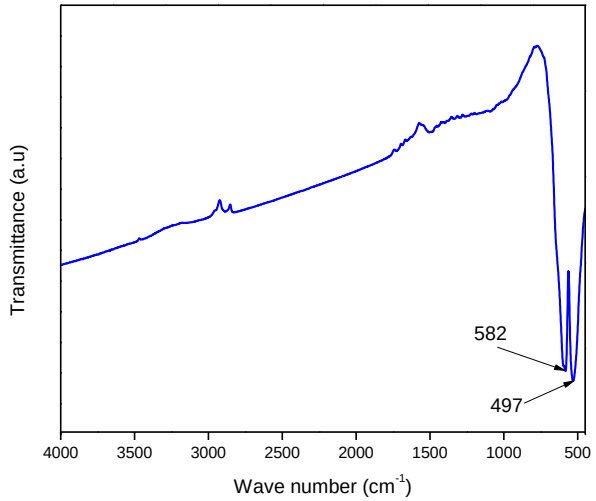


*Figure 1. FTIR Spectrum of NMO*

### *3.2. XRD Analysis*

The structure of the $NiMn_2O_4$ is analysed by XRD (Fig. 2). The diffraction peaks 18.1°, 24.73°, 29.11 33.72°, 36.6°, 42°, 50.65°, 55.1°, 63.94°, 65.8° and 72,28°corresponded to the (111), (200), (220),(311),(222) ,(400) ,(422),(511), (440),(531) and (533)diffraction planes, which can be indexed into the face- centred cubic phase of $NiMn_2O_4$. The obtained XRD patterns of NMO powders are well-matched with a face-centred cubic spinel crystal structure (JCPDS no. 71-0852) belonging to the space group Fd-3 m.

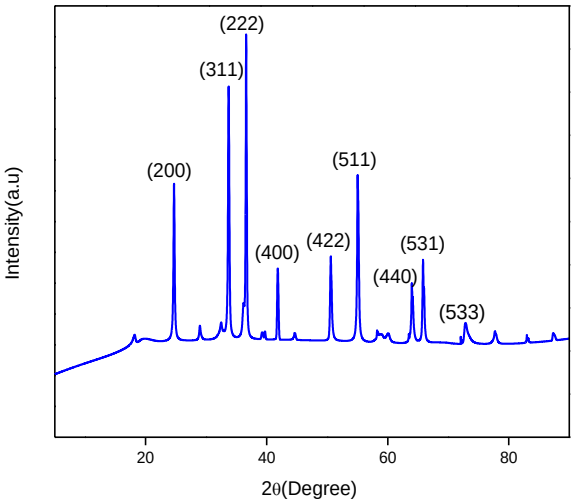


*Figure 2. XRD pattern of NMO*

### *3.3. XPS analysis*

The chemical composition of the prepared NMO is analysed by XPS. The narrow resolution survey spectrum (Fig 3a) of the synthesised material shows the presence of peaks of Ni, Mn, O and C elements. The signal peak of C element attributed to the foreign carbon contamination of material on exposure to atmosphere. The energy spectrum of Ni 2p (Fig. 3b) shows two spin–orbit peaks with the binding energies of 854 eV and 872 eV, corresponding to the peaks of Ni $2p^{3/2}$ and Ni $2p^{1/2}$ were assigned to the $Ni^{2+}$ state and two satellite half peaks around 861 and 879 eV, were assigned to the $Ni^{3+}$ state [19,20,21]. The Mn 2p spectrum peaks in Fig. 3c) show that the Mn 2p region consists of a spin–orbit doublet with Mn $2p^{1/2}$ and Mn $2p^{3/2}$ peaks with the binding energies of 653 eV and 641 eV, were assigned to the $Mn^{3+}$ and $Mn^{2+}$ states. The energy spectrum of O 1s (Fig.3d), the peaks located at 529 eV and 531 eV can be ascribed to the metal–O bond and the H–O–H bond, respectively [20,21]. Combined with XRD analysis it can be confirmed that the prepared product is pure spinel $NiMn_2O_4$.

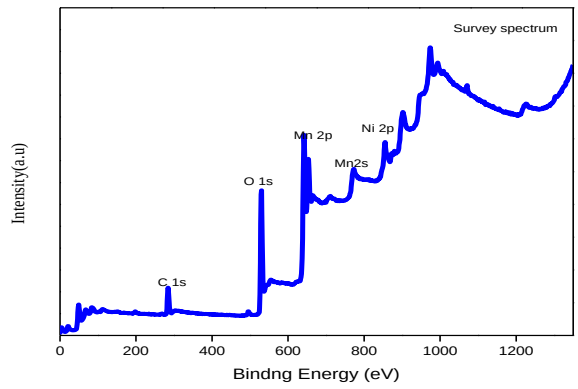


*3a)*

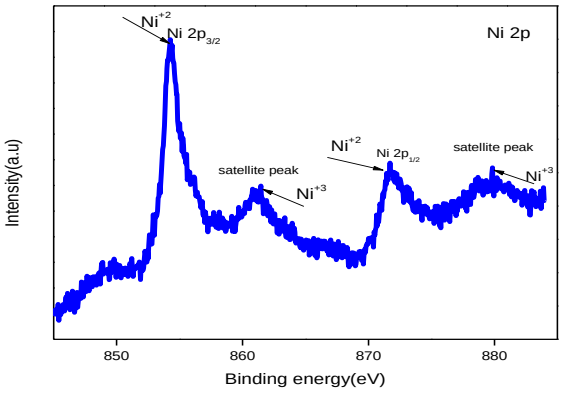


*3b)*

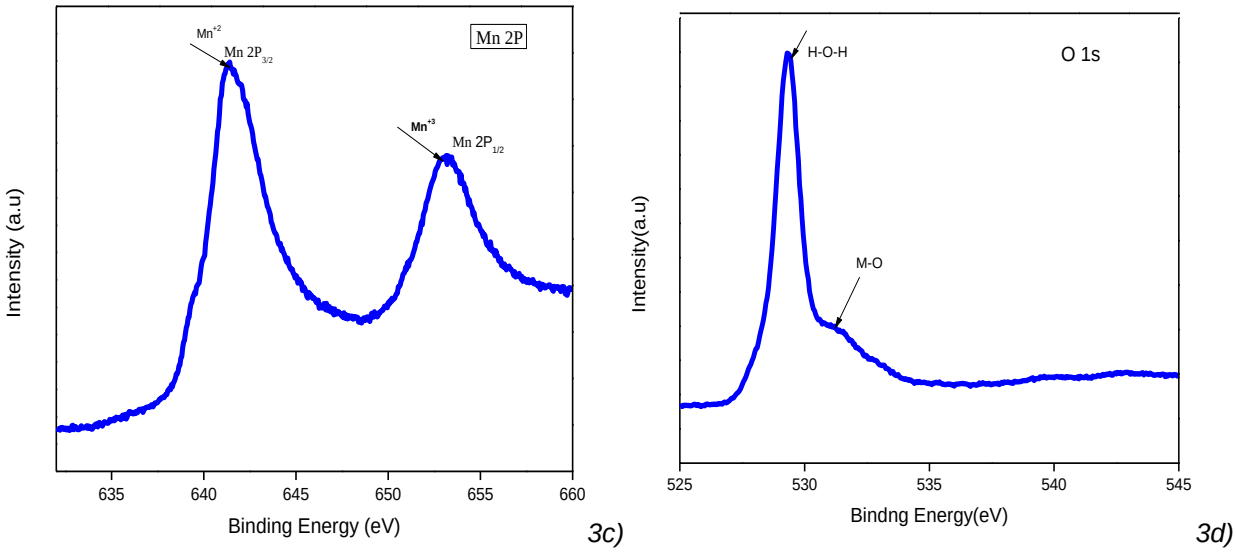


*Figure 3. XPS spectra for the as-prepared $NiMn_2O_4$: (a) a total survey, (b) Ni 2p, (c) Mn 2p, and (d) O 1s*

### *3.4. Brunauer-Emmett-Teller (BET)and Barrett-Joyner-Halenda (BJH) analyses*

BET analysis is performed to examine the specific surface area of the NMO. The specific surface area of the synthesised NMO is analysed by $N_2$ adsorption-desorption at 77K. The nitrogen adsorption-desorption isotherm for NMO is displayed in Fig 4 (a). From the BET analysis surface area was calculated to be 10.513 $m^2g^{-1}$. The pore size distribution of NMO is analysed through BJH (Barrett, Joyner, and Halenda) method and is displayed in Fig 4 (b). The average pore diameter of NMO was evaluated as 8.55nm in the mesoporous region of NMO. The mesoporous nature of the electrode material facilitates rapid charge transport across the electrode-electrolyte interface.

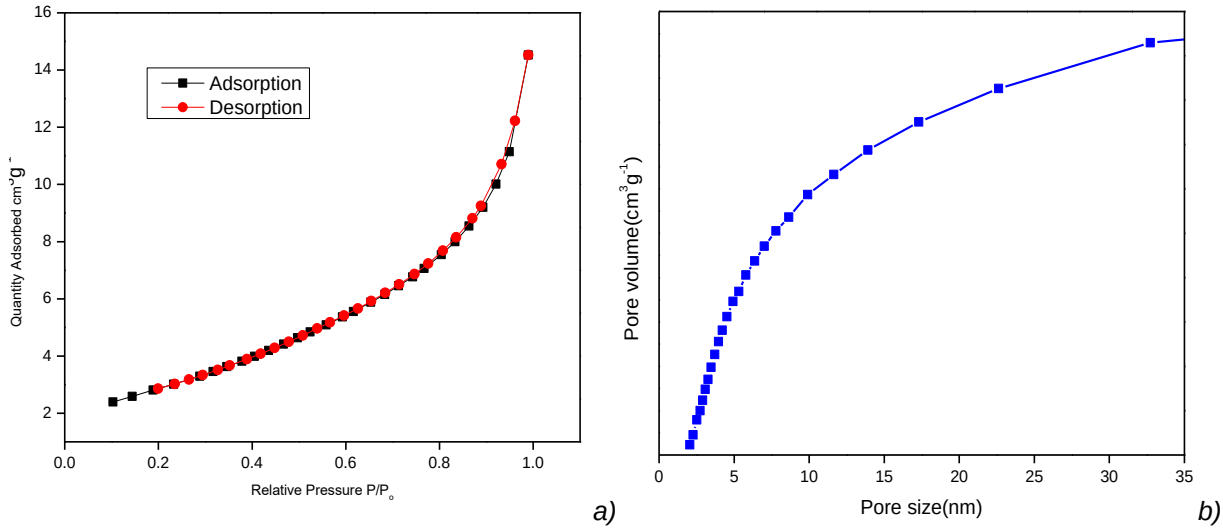


*Figure 4. a) BET Nitrogen adsorption-desorption isotherms of NMO, b) Pore size distribution curve of NMO*

### *3.5. Surface Morphology Analysis*

Surface morphology analysis of the synthesised electrode material is analysed using FE-SEM (Figure 5.) and it exhibited nano crystalline nature. The X-ray energy dispersive spectrum (EDAX) (Fig. 5(d)) confirms that the Ni, Mn and O elements at a molar ratio of 1: 2: 4 co-exist in the final product, which further confirms that the obtained product is $NiMn_2O_4$.

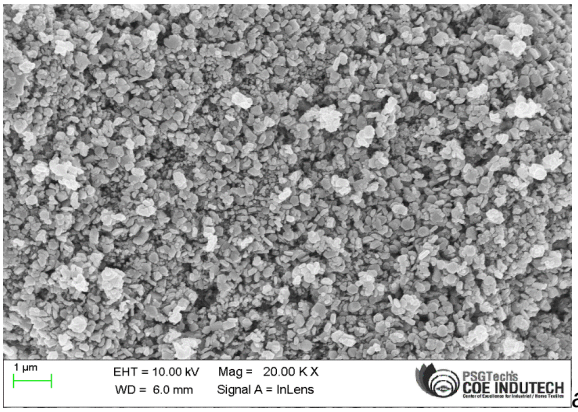


a)

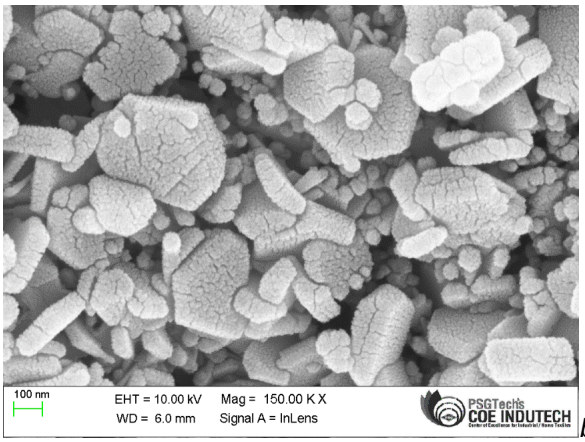


b)

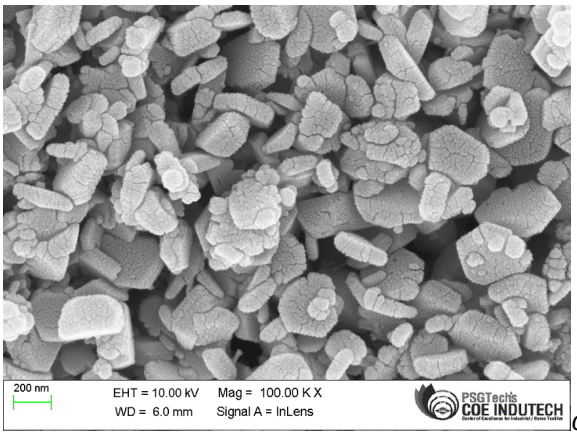


c)

*Figure 5. FE-SEM micrographs of the NMO at different magnification(a) (b)and (c)*

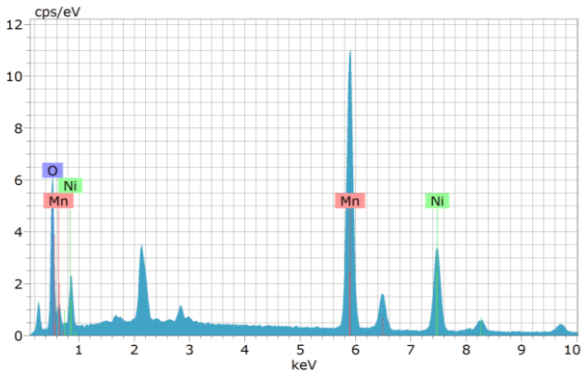


*Figure 5(d). EDAX spectrum of NMO*

### *3.6. Electrochemical characterizations*

#### 3.6.1 Cyclic voltammetry (CV)

The electrochemical performance of the as-prepared $NiMn_2O_4$ for supercapacitor applications was evaluated by cyclic voltammetry in various concentrations of KOH electrolyte (1M, 3M and 6M) at different scan rates, as shown in Fig. 6.

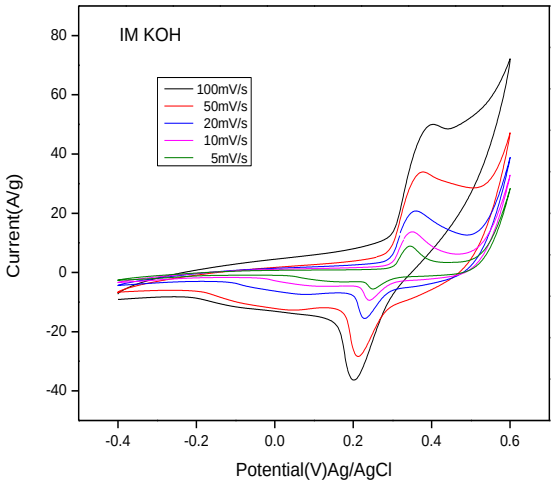


a)

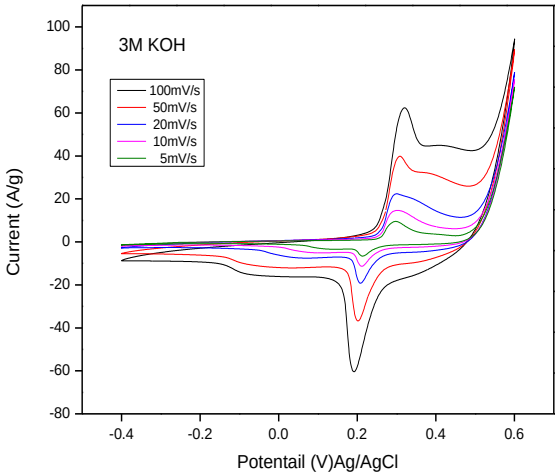


b)

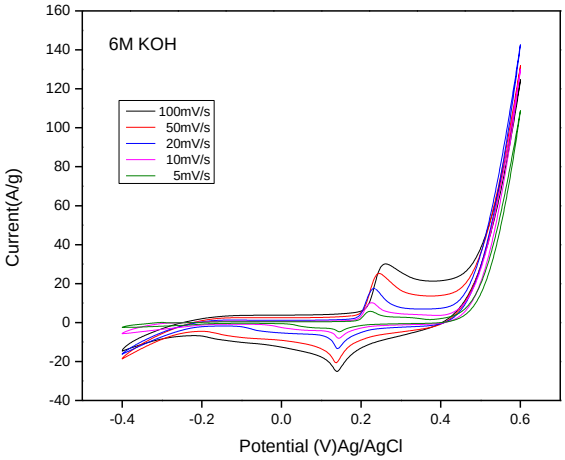


c)

*Figure.6. CV plot of NMO electrodes in (a)1M, (b)3M and (c)6MKOH electrolyte*

The presence of redox peaks in the CV plots of the $NiMn_2O_4$ electrodes is because of the faradic reactions taking place at the electrode–electrolyte interface [22]. CV curves exhibit reversibility and the current increases on increasing the scan rate. The electrochemical redox reactions of $NiMn_2O_4$ electrodes in KOH electrolytes are given equation (1) and (2)

$$NiMn_2O_4 + OH– + H_2O \leftrightarrow NiOOH + 2MnOOH + 2e^- \quad (1)$$

$$MnOOH + OH^- \leftrightarrow MnO_2 + H_2O + e^- \quad (2)$$

The Specific capacitance of $NiMn_2O_4$ electrodes is calculated by Equation (3)

$$C_s = \frac{\int_{v1}^{v2} i(v)dv}{(v2 - v1)ms} \quad (3)$$

where the numerator indicated the total charge enclosed by the CV curve, (v2 -v1) is the working potential window, m is the mass, and 's' is the scan rate.

The area under the CV curve is directly proportional to the specific capacitance of the electrode material. The specific capacitance of the NMO electrodes in 1 M KOH electrolyte is determined as 290.63, 218.99, 170.39, 115.96 and 89.33F/g for scan rate 5, 10, 20, 50 and 100 mV/s respectively. From CV curve it is seen that area of the CV curve of the NMO electrode in 6 M KOH is larger than that of 1 M and 3 M KOH. With an increase in the concentration of KOH electrolyte from 1 M to 6 M, the specific capacitance of the NMO electrode increases from 290.56 F/g to 751.57F/g at scan rate of 5mV/s. The slower scan rate allows slower process that takes a lot of time while the faster scan rate makes the process faster. However, higher capacitance is generally achieved at lower scan rates. This is because greater number of electrolyte ions can penetrate into the electrode pores for longer time at lower scan rates [23].

*Table1. Summarizes the specific capacitance values of the NMO electrode material determined from the CV plots at different scan rates in 1M, 3M and 6M KOH electrolyte*

| Scan rate(mV/s) | Specific Capacitance F/g | | |
|---|---|---|---|
| | 1M KOH | 3M KOH | 6M KOH |
| 5 | 290.63 | 470.98 | 751.57 |
| 10 | 218.99 | 305.05 | 521.65 |
| 20 | 170.39 | 208.11 | 363.45 |
| 50 | 115.96 | 135.03 | 164.18 |
| 100 | 89.33 | 95.98 | 101.60 |

Table1 summarizes the specific capacitance values of the NMO electrode material determined from the CV plots at scan rates of 100mV/s to 5mV/s in 1 M, 3M and 6 M KOH electrolyte. Fig.6. (d)displays the plot of specific capacitance the NMO electrode vs. scan rate, in 1 M, 3 M, and 6 M KOH. From the plot it reveals that lower scan rate has achieved higher specific capacitance and as the concentration of KOH increases from 1M to 6M specific capacitance also increases.

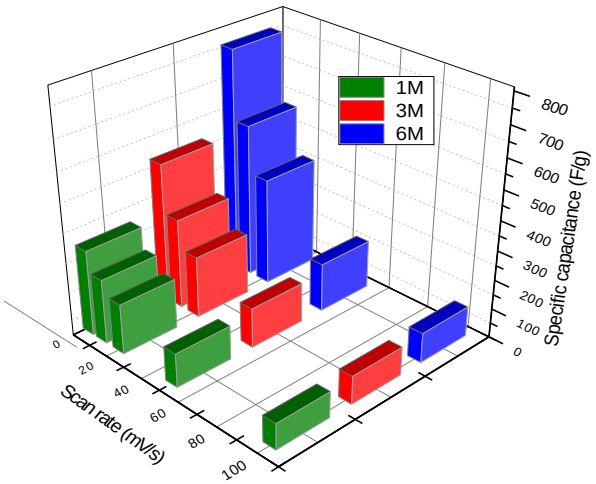


*Figure 6(d). Plot of specific capacitance the NMO electrode vs. scan rate, in 1 M, 3M, and 6 M KOH electrolyte*

3.6.2. Electrochemical impedance spectroscopy (EIS)

The electrochemical performance of the active material was further examined by EIS. This study has been performed for analysing resistance that occurs due to charge transportation and diffusion of active material. The Nyquist plot for NMO electrodes obtained in various concentrations of KOH (1M,3M and 6M) are shown in Fig.7. From the Nyquist plots, the semicircle at a high frequency and straight line at low frequency region are indicating the capacitive behaviour of the electrode material. The x- intercept with the starting curve at higher frequency region is called effective series resistance (Rs). It is usually exerted as a combination of ionic resistance in electrolyte, contact resistance of the active material to the current collector and the intrinsic resistance of the active material. The semicircle at high frequency region, implies the charge transfer resistance (Rct) at electrode electrolyte interface. The Rct value could be directly measured from the diameter of the semicircle [24]. The values of Rs and Rct evaluated from EIS study are 0.85Ω and 1.20Ω in 1M KOH, 0.57 Ω and 0.87 Ω in 3M KOH and 0.34 Ω and 0.42 Ω in 6M KOH electrolyte. The lower values of Rs

and Rct is obtained for electrode material in 6M KOH and NMO electrodes exhibit enhanced electrochemical performance in 6M KOH over 1M and 3M KOH.

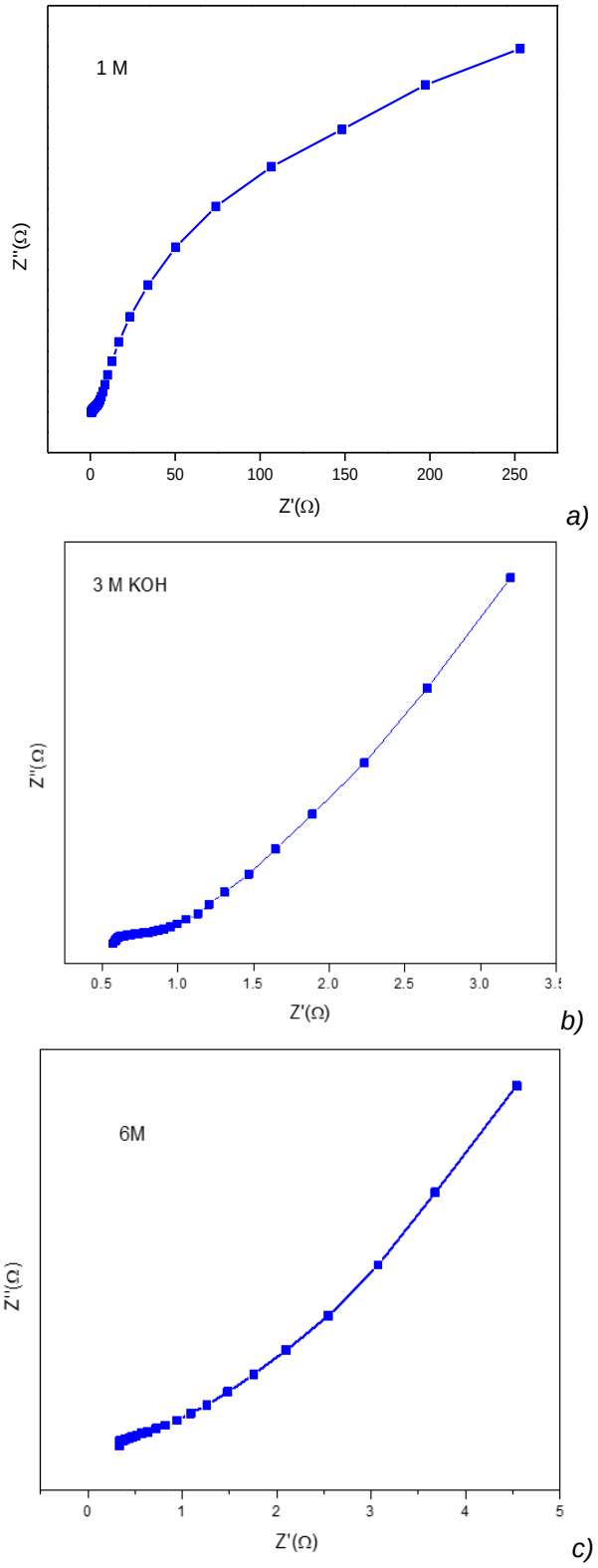


*Figure 7. EIS plot of NMO electrodes in a) 1M KOH b) 3M KOH and c) 6M KOH*

## 4. CONCLUSIONS

In the present work, $NiMn_2O_4$(NMO) nanoparticles are prepared by microwave assisted co-precipitation. The XRD study confirms the cubic spinel structure for $NiMn_2O_4$. The mesoporous nature of the NMO electrode material was confirmed through BET analysis with a specific surface area of 10.513 $m^2g^{-1}$and an average pore diameter of 8.55nm. The maximum specific capacitance of 751.57 F/g is obtained for electrode material in 6M KOH at scan rate of 5mV/s. The lower values of Rs and Rct is obtained for electrode material in 6M KOH and NMO electrodes exhibit enhanced electrochemical performance in 6M KOH. The results demonstrate that the spinel NMO NPs are promising candidates for fabricating efficient electrochemical capacitors.

*Acknowledgements*

For analytical support, the authors acknowledge the Centralized Common Instrumentation Facility (CCIF), Government College for Women, Thiruvananthapuram.

## 5. REFERENCES

[1] K., Ki-Hyun, W. Raza, E. E. Kwon, J. Yang, S. Kumar, A. Mehmood, N. Raza (2018) Recent Advancements in Supercapacitor Technology, Nano Energy., 52,441–473.
doi.org/10.1016/j.nanoen.2018.08.013.

[2] E.Prasad, H.S. Panda (2015) Synthesis and Characterization of NiCo $(OH)_2$ Material for Supercapacitor Application, IARJSET., 2 (9),10–13. doi:10.17148/IARJSET.2015.2903.

[3] L.Prasad, U. S. Chavan (2019) Surfactant- Assisted Cabbage Rose-like CuO Deposition on Cu Foam by for Supercapacitor Applications, Inorganic and Nano- Metal Chemistry., 1–7.
doi.org. /10.1080/24701556.2019.1569685.

[4] J.R. Miller, P.Simon (2008) Electrochemical capacitors for energy management, Science.,321(5889) 651-652.

[5] M.V. Kiamahalleh, S.H.S. Zein, G. Najafpour, S.A. Sata, S. Buniran (2012) Multiwalled carbon nanotubes-based nanocomposites for supercapacitors: a review of electrode materials, NANO: Brief Reports and Reviews.,7(2) 1-27,
doi: 10.1142/S1793292012300022.

[6] M.S. Halper, J.C. Ellenbogen (2006) Supercapacitors: A Brief Overview, The MITRE Corporation, McLean, Virginia, USA, (b)F. Ƀeguin, E. Frackowiak (Eds.), 2013Supercapacitors: Materials, Systems, and Applications, Wiley-VCH Verlag GmbH & Co. KGaA, Weinheim, Germany, (Chapter 2).

[7] P.P. Bhagwan, S. Shukla, S. Saxena (2016) Graphene Oxide – Polyvinyl Alcohol Nanocomposite Based Electrode Material for Supercapacitors, Journal of Power Sources., 321, 102–105. doi.org/10.1016/j.jpowsour.2016.04.127.

[8] M. Sanjoy, U. Rana, S. Malik (2017) Reduced Graphene Oxide/Fe3O4/Polyaniline Nanostructures as Electrode Materials for an All-Solid-State Hybrid Supercapacitor, Journal of Physical Chemistry C., 121 (14), 7573–83.doi.10.1021/acs.jpcc.6b10978.

[9] W. Huanhuan, J. Lin, Z. Xiang Shen (2016) Polyaniline (PANi) Based Electrode Materials for Energy Storage and Conversion. Journal of Science: Advanced Materials and Devices., 1 (3), 225–255.doi.org/10.1016/j.jsamd.2016.08.001.

[10] D.Yong-Qiang, R.Shao-Zhao, G. Liu, J. Cai, Y. Zhang, J. Qiu, B. Wei (2016) Electrochemical and Capacitive Properties of CarbonDots/Reduced Graphene Oxide Supercapacitors. Nanomaterials., 6(212),1-12. doi:10.3390/nano6110212.

[11] S. Mohapatra, A. Acharya, G.S. Roy, (2012) The role of nanomaterial for the design of supercapacitor, Latin-American Journal Physics Education., 6 (3), 380–384. www.lajpe.org.

[12] A. Ray, A. Roy, S. Saha, M. Ghosh, S. Roy, G. Chowdhury, T. Maiyalagan, S. Kumar Bhattacharya, D.Sachindranath (2019) Electrochemical Energy Storage Properties of Ni-Mn-Oxide Electrodes for Advance Asymmetric Supercapacitor Application. Langmuir., 35, 8257−8267.

doi.org/10.1021/acs.langmuir.9b00955.

[13] S. Deka (2023) Nanostructured mixed transition metal oxide spinels for supercapacitor application, Dalton Transactions.,52(4)

doi.org/10.1039/D2DT02733J.

[14] S. D. Dhas, A.Parvejha, S. Maldara, D.Meenal, A. Patil, R.M. Waikarb, R. G. Sonkawade, S. K. Chakarvarti, S. K. Shinde, D. Y. Kim, A. V. Moholkar (2021) Probing the electrochemical properties of $NiMn_2O_4$ nanoparticles as prominent electrode materials for supercapacitor applications, Materials Science & Engineering B., 27,115298.

https://doi.org/10.1016/j.mseb.2021.115298.

[15] S. Sahoo, S. Zhang, Sh.Jae-Jin (2016) Porous ternary High Performance Supercapacitor Electrode Based on reduced Graphene Oxide, $NiMn_2O_4$, and Polyaniline, Electrochimica Acta., 216, 386–396. doi.org/10.1016/j.electacta.2016.09.030.

[16] M.Zhang, S. Guo, L. Zheng, G. Zhang, Z. Hao, L. Kang, Z.H. Liu (2013) Preparation of NiMn2O4 with Large Specific Surface Area from an Epoxide-Driven Sol-Gel Process and Its Capacitance, ElectrochimicaActa.,87,546−553.

doi.org/10.1016/j.electacta.2012.09.085.

[17] H.Pang, J. Deng, S. Wang, S. Li, J. Du, J. Chen, J. Zhang (2012) Facile Synthesis of Porous Nickel Manganite Materials and Their Morphology Effect on Electrochemical Properties, RSC Advances., 2, 5930−5934. doi:10.1039/c2ra20245j.

[18] G. Ashcroft, I. Terry, R. Gover (2006) Study of the preparation conditions for NiMn2O4 grown from hydroxide precursors, Journal of the European. Ceramic society., 26 (6) 901–908.

doi: 10.1016/j.jeurceramsoc.2004.11.023.

[19] W. Kang, Y. Tang, W. Li, X. Yang, H. Xue, Q. Yang, C.-S. Lee (2015) High interfacial storage capability of porous NiMn2O4/C hierarchical tremella-like nanostructures as the lithium-ion battery anode. Nanoscale.,7, 225–231. doi: 10.1039/C4NR04031G

[20] S. Aouini, A. Bardaoui, D. M. F. Santos, R. Chtourou (2022) Hydrothermal synthesis of CuMn2O4 spinel-coated stainless-steel mesh as a supercapacitor electrode. Materials in Electronics., 16,12726-12733.
doi.org/10.1007/s10854-022-08219-4.

[21] Ji.Fang, Zh. Chen, W. Wei, Y. Li, T. Liu, Zh. Liu, Xi. Yue, Zh. Jiang (2015) A carbon fiber based three-phase heterostructures composite CF/Co0.2Fe2.8O4/PANI as an efficient electromagnetic wave absorber in Ku band, RSC Advances.,5, 24607–24614. doi: 10.1039/C5RA07192E.

[22] B. Senthilkumar, K. Sankar, L. Vasylechko, Y. Lee (2014) Selvan, Synthesis and electrochemical performances of maricite-NaMPO4 (M= Ni Co, Mn) electrodes for hybrid supercapacitors, RSC Advances., 4, 53192–53200.

doi: 10.1039/c4ra06050d.

[23] M.Arunkumar, A. Paul (2017) Importance of Electrode Preparation Methodologies in Supercapacitor Applications., ACS Omega., 2, 8039–8050.

doi.org/10.1021/acsomega.7b01275.

[24] P. Gao, P. Metz, T. Hey, Y. Gong, D. Liu, D.D. Edwards, J.Y. Howe, R. Huang, S. T. Misture (2017) The critical role of point defects in improving the specific capacitance of δ-$MnO_2$ nanosheets, Nature Communications., 8,14559,1-10.

doi:10.1038/ncomms14559.

## IZVOD

### SINTEZA $NiMn_2O_4$ KAO ELEKTRODNOG MATERIJALA ZA SUPER KONDENZATORSKE PRIMENE

*U ovom radu, spinel $NiMn_2O_4$ je uspešno sintetizovan metodom ko-precipitacije uz pomoć mikrotalasne pećnice, nakon čega je usledila kalcinacija na 500°C. Kristalna struktura i prisustvo funkcionalnih grupa u $NiMn_2O_4$ okarakterisani su difrakcijom rendgenskih zraka (XRD) i infracrvenom spektroskopijom Furijeove transformacije (FT-IR). Morfologija površine je ispitivana pomoću polja emisione skenirajuće elektronske mikroskopije (FE SEM). Iz BET analize izračunato je da površina površine i srednji prečnik pora mezoporoznih NMO nanočestica iznosi 10,513 m2g-1 i 8,55 nm. Elektrohemijske performanse materijala kao elektrodnog materijala za primenu u superkondenzatorima analizirane su cikličnom voltametrijom (CV) i spektroskopijom elektrohemijske impedanse (EIS). Specifični kapacitet NMO elektrode se povećao sa 290,56 F/g na 751,57 F/g sa povećanjem koncentracije sa IM KOH na 6M KOH pri brzini skeniranja od 5mV/s. Ovi rezultati ukazuju na spinel $NiMn_2O_4$ kao kandidata koji obećava za aplikacije za **skladištenje energije visokih performansi.***

***Ključne reči:*** *Mikrotalasna metoda, spinel, $NiMn_2O_4$, elektrohemijske performanse, specifična kapacitivnost*

*Naučni rad*
*Rad primljen: 25.02.2024.*
*Rad korigovan: 12.05.2024.*
*Rad prihvaćen: 27.05.2024.*
*Rad je dostupan na sajtu: www.idk.org.rs/casopis*

Paulcy Rani Palayyan Raja Bai https://orcid.org/:0009-0003-4200-1474
Vaishnavi Sreekala Kumari Gopakumar https://orcid.org/:0009-0005-2104-6619
Sivakala Sarojam https://orcid.org/:0000-0002-2126-1790
Anu Mini Aravind https://orcid.org/:0000-0002-2941-208X
Xavier Thankappan Suryabai https://orcid.org/:0000-0001-8955-0743